DALTON
FULL PAPER

Structural aspects and thermal properties of takovite-like layered double hydroxides pillared with chromium oxo-anions

François Malherbe,*† Laurent Bigey, Claude Forano, André de Roy and Jean-Pierre Besse

Laboratoire des Matériaux Inorganiques, Université Blaise Pascal, 24, avenue des Landais, 63177 Aubiere Cedex, France

Received 11th May 1999, Accepted 6th September 1999

Intercalated layered double hydroxides (LDHs) of chromate (CrO_4^{2-}) and dichromate ($Cr_2O_7^{2-}$) have been synthesised and characterised. The parent chloride material ([Ni–Al–Cl]) was obtained by coprecipitation at constant pH and further anion-exchanged to incorporate the desired oxo-anions. The physico-chemical properties of all compounds were investigated using X-ray powder diffraction, infrared spectroscopy, thermogravimetric analyses and extended X-ray absorption spectroscopy (EXAFS). The structural evolution of the pristine and pillared materials, following calcination between 100 to 450 °C, was also thoroughly studied. It is shown that the intercalated guests, chromate and dichromate anions, interact with the host hydroxylated sheets at moderate temperatures. This so-called "grafting process" is characterised by a reorganisation of the anionic species within the interlamellar domain associated with a shrinking of the basal spacing. This phenomenon was clearly evidenced with powder X-ray diffraction (contraction of the interlamellar distance) and, more interestingly, by chromium K-edge EXAFS (variation in the local environment of the probe element). On the other hand, thermogravimetric studies indicated that the thermal stability was greatly enhanced following pillaring with oxo-anions. This is reflected through the dehydroxylation step of the LDHs sheets which shifted to much higher temperatures, from 280 °C in the [Ni–Al–Cl] precursor to over 450 °C in the dichromate intercalated compound. Rehydration and reverse exchanges with carbonate anions of the thermally treated materials were both unsuccessful, suggesting that the grafting phenomenon is irreversible. The specific surface areas were also negatively affected following anion exchange and moderate thermal treatment, indicating that the structural changes observed through the different analytical techniques also influence the microtextural properties.

Introduction

Layered double hydroxides (LDHs) are materials of increasing interest because of their potential use in various fields such as pharmaceuticals, adsorbents, sensors, *etc.*, and mostly in the area of catalysis.[1] They constitute a class of layered compounds, resembling the naturally occurring hydrotalcite,[2] and are generally described by the empirical formula $[M^{2+}_{1-x}M^{3+}_{x}(OH)_2]A^{m-}_{x/m}\cdot nH_2O$, abbreviated hereafter as $[M^{2+}-M^{3+}-A]$, where x may vary from 0.17 to 0.33; A represents the m-valent anion necessary to compensate the net positive charge.

One of the most important properties of LDHs is based on their high anion exchange capacities: a value of 250 m equivalents per 100 g of dried material has been reported for a zinc–aluminium LDH.[3] The primary objective of anion exchange is to modify the chemical composition of LDHs, mainly through the incorporation of those elements that cannot enter in the composition of the brucite-like sheets, and also to have a combination of different potentially active species to induce a synergetic effect. Also, it has been shown that the contribution to catalytic activity of a particular element can be different whether this element is originally present in the brucite-like sheets or as an intercalate.[4] A large number of organic and inorganic anions intercalated in LDHs have been reported, giving a very good insight into this specific property.[5] However, one major drawback to the technological utilisation of layered double hydroxides, as compared to other similar structures like zeolites or cationic clays, is associated to their thermal instability. Their resistance to thermal decomposition is usually low and their use as lamellar materials in high temperature applications is often impeded by this.

Another significant characteristic of lamellar compounds is the presence of micro- or meso-porosity that imparts the solid with a series of desirable properties. For example, some authors have explained observed differences in reactivity and selectivity by the effect of the pore structure on the diffusion of reactants.[6] The specific surface areas of as-synthesized hydrotalcite-like compounds are known to be relatively low (around 30–60 $m^2\ g^{-1}$) compared, for instance, to those of zeolites, *e.g.* for Na–Y a value of 715 $m^2\ g^{-1}$ is reported.[7] However, we have shown[8] that the use of organic media during synthesis or regeneration of calcined phases can enhance significantly the surface and porosity properties of synthetic hydrotalcite. Attempts to improve both the thermal and surface properties of LDHs have been realised through the intercalation of polyoxometalates[9] to mimic the pillaring effects achieved in cationic clays. Apart from improvement of the structural properties, oxo-anions generally confer LDHs with redox as well as bifunctional acid–base properties: the basic sites are located on the hydroxylated brucite-like sheets while the acid sites are borne by the metalate pillars.[10]

In the present work we report on the preparation and properties of chromate and dichromate intercalated [Ni–Al] LDHs. The structural changes following thermal treatment were studied using powder X-ray diffraction (PXRD), TGA-DTA, X-ray absorption and nitrogen adsorption. The catalytic properties of these materials, thermally activated at 450 °C, have been investigated elsewhere[11] in the oxidative dehydrogenation of ethylbenzene.

† *Present address*: Chemistry Department, Monash University, Wellington Road, Clayton, Victoria 3168, Australia. E-mail: malherbe@sci.monash.edu.au

Table 1 Chemical composition of [Ni–Al–Cl] and the derived chromate and dichromate phases

Parameter	[Ni–Al–Cl]	[Ni–Al–CrO_4]	[Ni–Al–Cr_2O_7]
Ni : Al (molar ratio)	2.91	2.88	2.83
x (degree of substitution)	0.256	0.258	0.264
Anion (moles per unit cell)	1.92	0.95	0.92
CO_3^{2-} (moles per unit cell)	0.14	0.05	0.00
Residual chloride ions (moles per unit cell)	—	0.02	0.25
$(\Sigma n[A_i^{n-}]) : [Al^{3+}]$ (molar ratio)[a]	1.04	1.02	1.05
Effective anion intercalation[b](%)	—	95.3	92

[a] Sum of all negative charges over the net positive charge (imposed by the amount of Al^{3+}). [b] Based on idealised formula derived from the Ni : Al atomic ratio.

Experimental

(a) Materials

Commercial materials were of reagent grade and used without further purification. A [Ni–Al–Cl] LDH was prepared by coprecipitation at constant pH according to previously published procedures,[12] using a mixture of 0.75 M $NiCl_2 \cdot 6H_2O$ and 0.25 M $AlCl_3 \cdot 6H_2O$. A [Ni–Al–CrO_4] layered double hydroxide was prepared following a procedure analogous to that described by de Roy and co-workers.[13] The exchange reaction was carried out without pH control due to the basicity of the LDH slurry. The dichromate-intercalated takovite [Ni–Al–Cr_2O_7] was prepared according to Depège *et al.*[14] The procedures were much the same as above except that here the pH was monitored and maintained at 6 by controlled addition of 1 M HCl.

(b) Methods

X-Ray powder diffraction analysis. All takovite-like materials were examined by powder XRD with a Siemens D501 diffractometer using Cu-Kα radiation. The samples were scanned from 2 to 76° (2θ) in steps of 0.08° with a count time of 4 s at each point.

FTIR spectroscopy. The IR spectra were recorded on a Perkin-Elmer 2000 FT spectrometer at a resolution of 2 cm^{-1} and averaging ten scans in the 400–4000 cm^{-1} region using the KBr pellet technique. A typical pellet contained *ca.* 1 wt.% sample in KBr.

Elemental analysis. Chemical analyses were performed by inductively coupled plasma (ICP) emission spectroscopy at the Analysis Centre of the CNRS, Vernaison.

Thermogravimetric analyses. Thermogravimetric analysis (TGA) was performed on a SETARAM thermogravimetric analyser. The samples were heated between 25 and 1050 °C under continuous airflow at a heating rate of 5 °C min^{-1} for all data collection.

X-Ray absorption spectroscopy. The XAS data were recorded in the transmission mode at the LURE (Orsay, France). Experiments were done near the nickel and chromium K edge at room temperature and 8 K. A step-by-step technique was used over a 1000 eV interval, with 2 eV steps and 1 s accumulation time. The data were processed using the single scattering formulae developed by Sayers *et al.*[15,16] and software elaborated by Michalowicz.[17]

Surface area and porosity measurements. The nitrogen adsorption–desorption isotherms were recorded at liquid nitrogen temperature on a Fison SP1920 instrument. The materials were pre-treated as follows: heating in air at 100 °C for 16 h followed by degassing for 4 h at 80 °C. Pore size distributions were calculated using the Barret–Joyner–Halenda (BJH) model on the desorption branch.

Results and discussion

Characterisation of the fresh samples

Results of chemical analyses for the parent and anion exchanged LDHs are given in Table 1. The Ni : Al atomic ratios in the coprecipitated solids are close to the solution values with some deviations in the exchanged materials. A loss of nickel through partial dissolution of the brucite-like sheets is not to be excluded during the anion exchange process. We can also note a slight contamination of [Ni–Al–Cl] and [Ni–Al–CrO_4] with carbonate ions, which is believed to occur during the washing/centrifuging cycles. However, this is not observed with the dichromate exchanged LDH owing to the acidity of the reaction mixture. Given that HCl is added to maintain a constant pH value (5.5–6.0), the presence of extra chloride ions implies a competition with the dichromate anion, the main consequence being a lower intercalation percentage. This competition between monovalent and divalent anions has been studied by Châtelet *et al.*,[18] showing a dependence on the solubility properties of the anions.

The effective anion intercalation, based on the Ni : Al ratio of the final compound, indicates an excess of negative charges: the ratio of all anions to the amount of aluminium is ideally equal to one. This results mainly from adsorption of anions on the crystallites, the incoming anion and/or carbonates. The relative amounts (in moles) of the different anions are given per unit cell, by reference to hydrotalcite whose structural formula is given as $[Mg_6Al_2(OH)_{16}]CO_3 \cdot 4H_2O$. The advantage is that the determination of the extent of anion exchange becomes relatively straightforward.

The X-ray powder diffraction patterns of [Ni–Al–Cl] and the exchanged phases are shown in Fig. 1. We have also summarised in Table 2 the main crystallographic parameters that can be derived from these analyses. Assuming a structure similar to that of hydrotalcite, the peaks can be indexed in a $R\bar{3}M$ symmetry with the interlamellar distance $d_{(003)}$ being equal to $c/3$ while the intermetallic distance is derived from the (110) diffraction line $a = 2d_{(110)}$. The pattern of [Ni–Al–Cl] exhibits a relatively sharp symmetric set of (00l) reflections indicative of a long range ordering in the stacking dimension. The analogous peaks for the exchanged materials are less intense and much broader, indicating a less organised stacking arrangement. This broadening of the diffraction peaks following anion exchange has been explained by various authors [19,20] as being the result of a disturbance in the structure due to the size of the incoming anions or to different aggregation mechanisms.[21] The particle size (Table 1) is an alternative way to point out the loss of crystallinity following anionic exchange. Given the results of elemental analysis and the relatively high crystallinity of the chloride precursor, we can tentatively assign a chemical formula for this compound: $[Ni_{5.92}Al_{2.08}(OH)_{16}]Cl_{1.92}(CO_3)_{0.08} \cdot 4.26H_2O$. Although the elemental compositions of the exchanged materials are very close to those for a hydrotalcite-like compound, for obvious reasons of poor crystallinity, there has been no attempt to derive a chemical formula. The expansion

Table 2 Crystallographic parameters of the parent and anion exchanged takovite-like LDHs

Sample	2θ/° of main peaks (0 0 3)	(0 0 6)	(1 1 0)	Basal spacing/Å (c/3)	Intermetallic distance/Å ($2a$)	Domain size[a]/Å
[Ni–Al–Cl]	11.03	22.35	60.79	8.01	3.04	1215
[Ni–Al–CrO_4]	10.78	21.72	60.79	8.19	3.04	403
[Ni–Al–Cr_2O_7]	9.39	19.01	60.79	9.42	3.04	556

[a] Using the Scherrer equation.

Table 3 Absorption bands (cm^{-1}) of the chromate and dichromate anions for: (1) crystalline state, (2) the respective potassium salt and (3) intercalated [Ni–Al] LDHs

Chromate	Symmetry T_d	Band assignments ν_d(Cr–O)	ν_{sym}(Cr–O)	δ_d(Cr–O)	δ_d(Cr–O)		
(1) Free anion[a]		890	*846*[b]	*349*[b]	378		
(2) K_2CrO_4		890	—	—	—		
(3) Interlayer		867	—	—	—		
Dichromate	C_{2v}	ν_{asym}(Cr–O)		ν_{asym}(Cr–O)		ν(Cr–O–Cr)	δ(Cr–O–Cr)
(1) Free anion[c]		966	935	905	893	764	560
(2) $K_2Cr_2O_7$		962	942	902	884	795, 772, 757	559
(3) Interlayer		948	939	910	880	743	—

[a] Nakamoto.[23] [b] Raman active only. [c] Calculated frequencies for the dichloromate anion from Brown and Ross.[24]

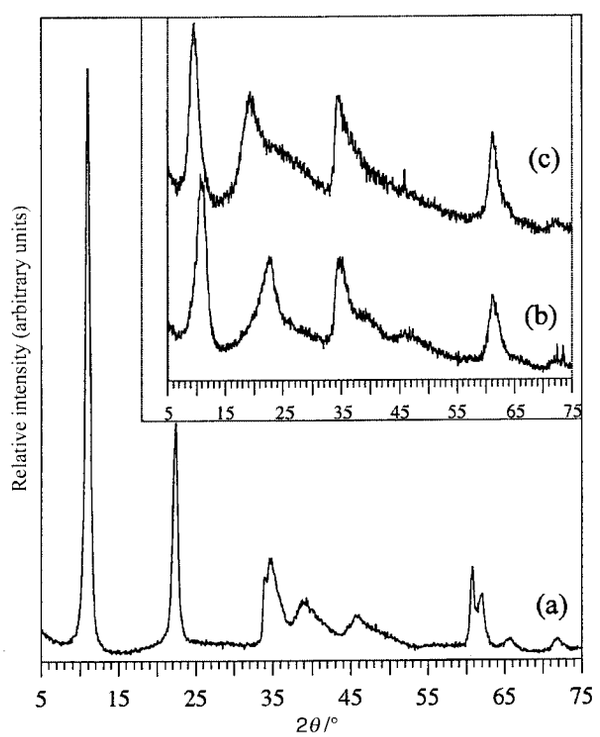

Fig. 1 XRPD patterns of (a) [Ni–Al–Cl], (b) [Ni–Al–CrO_4] and (c) [Ni–Al–Cr_2O_7] takovite-like LDHs.

of basal spacing observed with the chromate and dichromate strongly suggests the presence of these entities within the interlamellar domain.

The FTIR absorption spectra of the starting chloride LDH together with its intercalated derivatives are illustrated in Fig. 2. The set of characteristic bands at around 3480, 1624 and 1300 cm^{-1} correspond to the ν_{OH} stretching, ν_{OH} bending and ν_3 carbonate stretching vibrations. The relative width of this band has been associated with a disorganised interlamellar domain,[22] which seems to corroborate the XRD patterns. We can also note the absence of CO_3^{2-} contamination

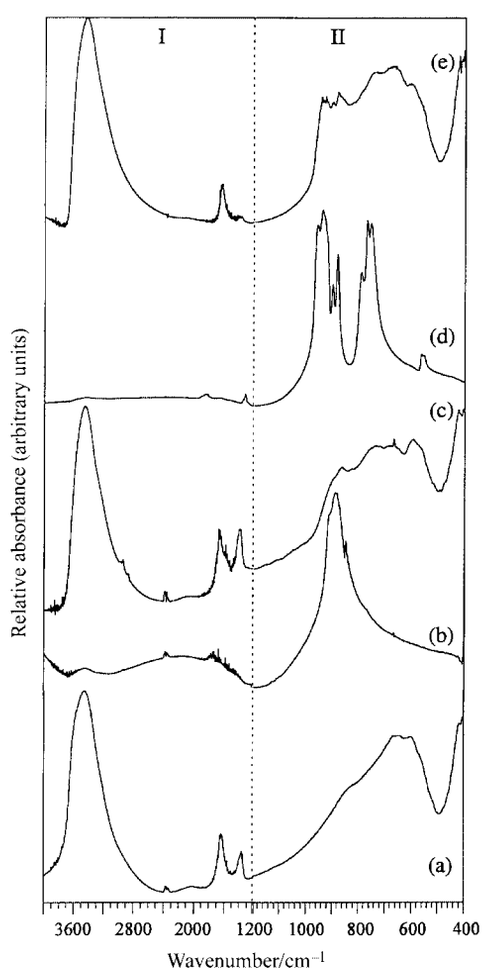

Fig. 2 Infrared of (a) the parent LDH, (b) potassium chromate, (c) chromate exchanged [Ni–Al], (d) potassium dichromate and (e) the dichromate intercalated [Ni–Al].

in the dichromate intercalated LDH. We have summarised in Table 3 the main absorbance bands observed in the exchanged

Table 4 Structural parameters for the different LDHs derived from X-ray absorption at the nickel K edge

LDH	Shell	Co-ordination number	r/Å	$2\sigma^2$ [a]/Å^2
[Ni–Al–Cl]	1st (oxygen)	6	2.06	0.078
	2nd (metal) [b]	6	3.07	0.086
[Ni–Al–CrO_4]	1st (oxygen)	6	2.06	0.080
	2nd (metal) [b]	6	3.07	0.088
[Ni–Al–Cr_2O_7]	1st (oxygen)	6	2.06	0.078
	2nd (metal) [b]	6	3.07	0.086

[a] Debye–Waller factor σ = root-mean-square internuclear separation. [b] No distinctions were made between Ni–Al and Ni–Ni at this level.

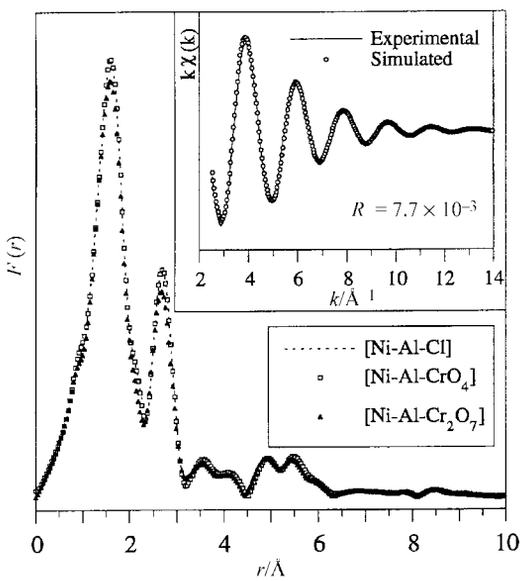

Fig. 3 X-Ray absorption spectra (EXAFS) of the as-synthesized LDHs. The inset shows the Fourier transformed simulation for [Ni–Al–Cl].

LDHs and starting potassium salts, together with the fundamental frequencies of the respective anions as per literature values.[23,24]

With reference to Nakamoto,[23] the only visible absorption band of CrO_4^{2-}, centred at 867 cm^{-1}, is assigned to the stretching frequency ν(Cr–O). The significant shift (23 cm^{-1}) of this band towards lower frequencies, indicating a weakening of the Cr–O bond, can be explained by an interaction *via* hydrogen bonds, either with the water molecules present in the interlamellar space or with the OH groups from the brucite-like sheets. The spectra of the dichromate species have been compared to those in a study of this anion by Brown and coworkers.[24,25] In the spectral window ranging from 800 to 400 cm^{-1}, where the strong lattice vibrations of the layered double hydroxides are normally found, it is rather difficult to assign specifically the vibration modes for ν(Cr–O–Cr). One broad band centred at 743 cm^{-1}, not visible in the chloride precursor, is nevertheless ascribed here to this vibration mode. Here also, the slight shift of the terminal Cr–O towards lower frequencies suggests the existence of hydrogen bonding.

The Fourier transform spectra of the materials at the nickel K edge are presented in Fig. 3 and the different structural parameters derived from these analyses are summarised in Table 4. For all three samples, the composition of the first peak is visibly very close given the good superposition of the spectra. This first shell corresponds to the octahedral environment of nickel, surrounded by the six OH groups, and the second reflects the contribution of heavier atoms, aluminium and/or nickel. As in these compounds no ordered distribution of the metals has been evidenced by X-ray diffraction, there were no attempts to resolve the exact nature of these atoms. The two fused peaks appearing between 5 and 6 Å are most probably due to the other atoms in the brucite-like sheets, rather than the interlamellar species, as no evolution in either their position or intensity is observed in the exchanged LDHs. Also, this value corresponds to approximately twice the intermetallic distance. However, their weak intensity and irregular shape, together with the existence of important multi-diffusion phenomena with increasing distance, hampered further simulation. One interesting observation that can be made is that the intercalation of anionic species does not seem to disturb the original arrangement in the brucite-like sheets. The nickel–oxygen and nickel–metal distances are in good agreement with values reported concerning takovite-like LDHs.[26]

The collation of the results from these various analytical tools seems to confirm the presence of the desired charge balancing anionic species within the interlamellar region. The next step in this work is to study the influence of these anions on the thermal properties and structure of synthetic takovite-like compounds.

Analysis of thermal behaviour

The X-ray powder diffraction patterns of the LDHs calcined between 100 and 450 °C are reproduced in Fig. 4. All the samples were calcined at the designated temperature for 16 h under ambient conditions and analysed without prior cooling. While the chloride LDH collapses quite rapidly at around 200 °C, the chromate and dichromate takovites are revealed to be much more stable, even after a prolonged calcination at 400 °C. With the pillared takovites, the slightly higher stability observed for the dichromate may result from the combined effect of the structural characteristics of the anion and the chromium loading, which is theoretically twice that of [Ni–Al–CrO_4]. However, the role of the pillar is not merely physically to support the layered framework, as the LDH structure is primarily conditioned by the presence of the hydroxylated sheets. When considering the thermal stability of the chloride LDH it is obvious that the hydroxide groups are eliminated at 200 °C, which is somehow associated to the relative stability of $Ni(OH)_2$, 230 °C, and $Al(OH)_3$, 300 °C. It seems that, in the pillared materials, the presence of the chromium oxo-anions hinders the condensation process which normally leads to destruction of the lamellar structure.

Fig. 5 shows the contraction of the basal spacing as a function of the calcination temperature. One important point is that, given the extent of the interlayer contraction, dehydration alone cannot account for the extremely low distances observed. On the other hand, no significant interlayer contraction was observed with the chloride LDH, the variation being at most 0.05 Å, attributed mainly to the loss of interlamellar water molecules, while in [Ni–Al–Cr_2O_7] the maximum decrease is 2.01 Å. There is a marked difference in the behaviour of the two exchanged materials; while in [Ni–Al–CrO_4] the interlayer contraction is gradual, in the dichromate LDH there is a considerable shrinkage at 100 °C (≈1.7 Å). However, both LDHs exhibit the same interlamellar spacing at temperatures equal to and above 250 °C, suggesting that the two anions might adopt identical orientations. The same behaviour of layered double hydroxides pillared with oxo-anions has been reported, *e.g.* CrO_4^{2-} in [Zn–Cr][13] LDHs, $Cr_2O_7^{2-}$ in [Cu–Cr][14] and SO_4^{2-} in [Mg–Al].[27] The authors all suggested the existence of a grafting process, mainly on the basis of the contraction of the basal spacing evidenced by X-ray diffraction. We have in this work extended the characterisation to a variety of analytical techniques to verify if this phenomenon can be evidenced by other means.

The TGA and DTG profiles for the three samples are shown in Fig. 6. The thermal decomposition of hydrotalcite-like

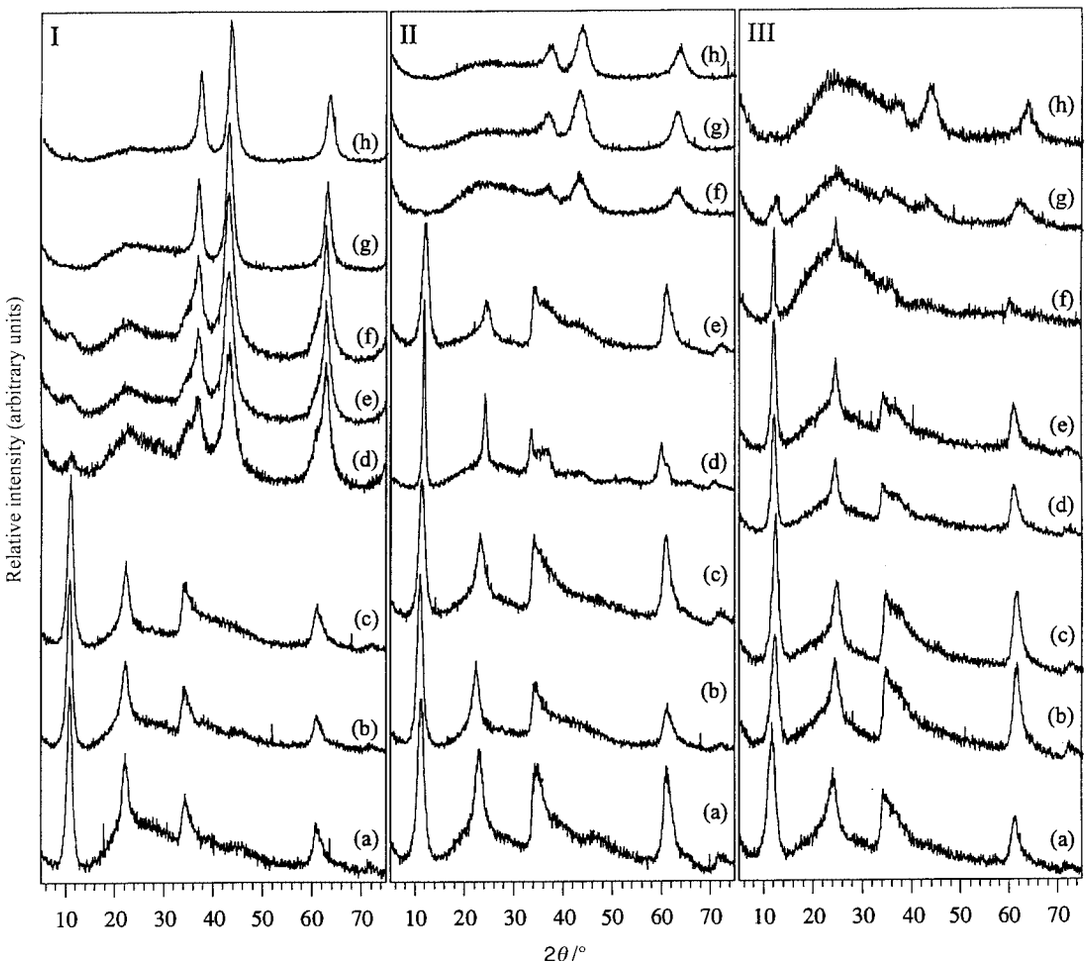

Fig. 4 XRPD patterns of (I) [Ni–Al–Cl], (II) [Ni–Al–CrO_4] and (III) [Ni–Al–Cr_2O_7] calcined at (a) 100, (b) 150, (c) 200, (d) 250, (e) 300, (f) 350, (g) 400 and (h) 450 °C.

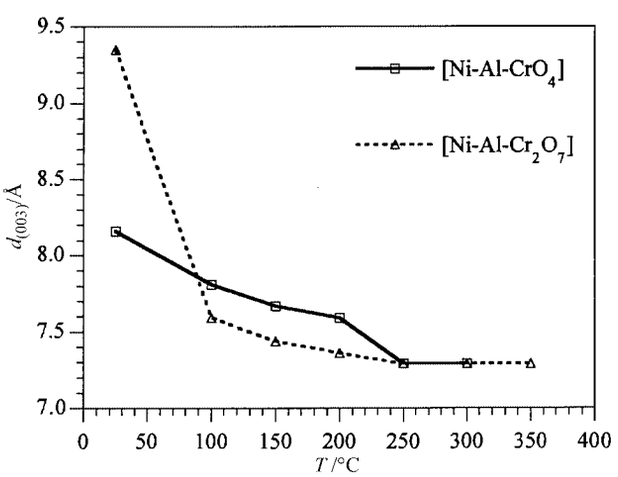

Fig. 5 Evolution of the interlamellar distance (d_{003}) as a function of the calcination temperature.

compounds has extensively been studied.[27–30] It is generally agreed that these materials tend to decompose in three distinct steps: loss of water molecules (adsorbed and intercalated), dehydroxylation for the brucite-like sheets and either loss of the anion (for volatile species like Cl^-, NO_3^- or CO_3^{2-}) or, for non-volatile species, inclusion of the metallic part in the formation of mixed metal oxides (*e.g.* CrO_4^{2-}, $Cr_2O_7^{2-}$, $V_2O_7^{2-}$). Concerning the first weight loss, the DTA profiles show a slight shift towards higher temperatures. In the chloride precursor the maximum loss is centred at 130 °C while for the exchanged LDHs this elimination peaks at 165 °C for [Ni–Al–Cr_2O_7] and 175 °C for [Ni–Al–CrO_4]. The shape of this first minimum gives an indication of the kinetics involved in the elimination of water molecules: in [Ni–Al–Cl] there is no marked separation between adsorbed and interlamellar water, suggesting that the process occurs in a slow and continuous way. On the other hand, in the anion exchanged materials, the DTG curves show a smooth loss up to 120 °C, which then changes into an abrupt slope for the departure of the intercalated water at a higher temperature. It is believed this is due to the possible interaction with the anionic species as well as the occupancy of the interlamellar domain.

In terms of the occupancy of the interlayer, it is easily imagined how the charge of the respective anion will dictate its density per unit volume while its geometry will influence its orientation. During the first minutes of the thermogravimetric analysis there is most probably a rearrangement of the interlamellar species: the water molecules and anions become more dynamic with increasing temperature. Owing to their spherical geometry the halogen anions are not affected by an eventual reorganisation, in contrast to the oxo-anions which can undoubtedly adopt different orientations. The loss of interlayer water molecules can therefore be hindered by the presence of obstacles defined by the anions and can thus get trapped between these entities. To simplify our viewpoint on the possible interactions of interlamellar water with the anions, the problem can be set the other way round: elimination of water is essentially determined by its boiling point. The existence of hydrogen bonds will greatly influence the intrinsic properties of the interlamellar water. The strength of hydrogen bonds is determined by the element, or more precisely its electronegativity, to which the hydrogen is linked, and the stronger the

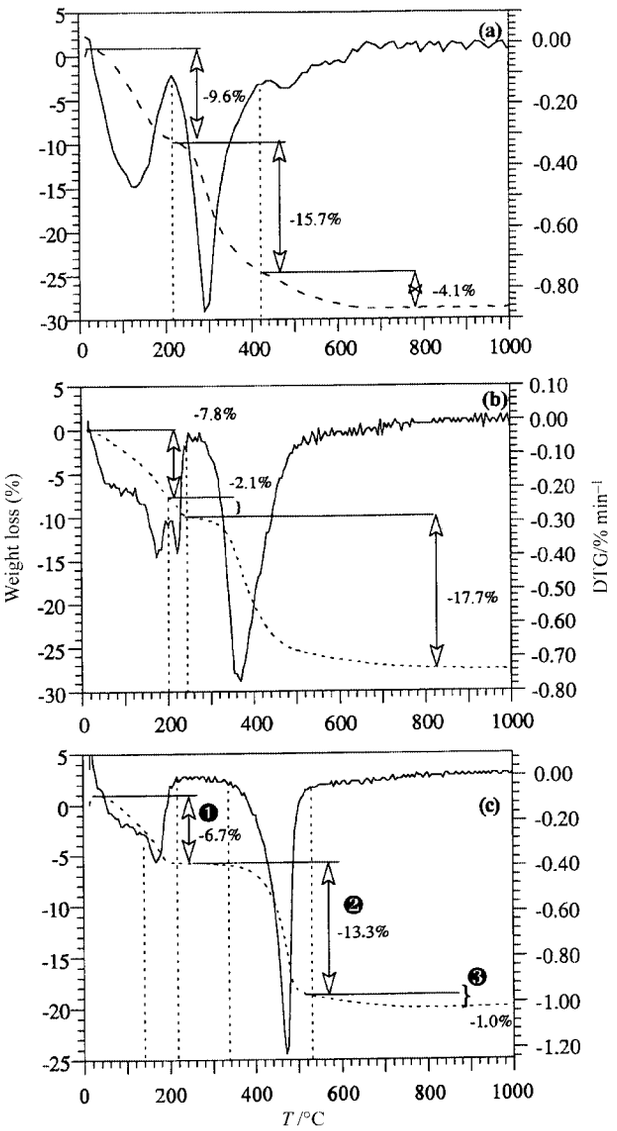

Fig. 6 Thermogravimetric analyses of (a) [Ni–Al–Cl], (b) [Ni–Al–CrO_4] and (c) [Ni–Al–Cr_2O_7].

bond the more difficult it would be to eliminate the water. The interlayer water molecules inevitably solvate the anions and this might partly explain the shift towards higher temperatures, the extent of which will depend on the nature of the anion. In the chloride form, hydrogen bonding with the chloride ions is expected to be much weaker than the bonding with the oxygen of the chromate and dichromate.

There is moreover a peculiarity in the behaviour of the chromate exchanged LDH: the peak ascribed to loss of interlamellar water is doubled, with two minima at 175 and 210 °C. A similar evolution has been reported for LDHs intercalated with the decavanadate anion, for example [Ni–Al][31] and [Zn–Cr],[32] which the authors attributed to the removal of differently held hydroxyl groups. However, when considering the TGA/DTG profiles of the chloride precursor, it is clear that the dehydroxylation process starts only at around 210 °C, with the maximum loss being at 290 °C. It is thus difficult in the case of the chromate-intercalated [Ni–Al] to assign this second minimum in the DTA specifically to partial dehydroxylation, in which case the same phenomenon should be also visible in the dichromate LDH. Some possible explanations for this observation are as follows.

The existence, within the interlamellar domain, of two types of interactions involving the water molecules: loosely bound ones through weak van der Waals forces and those hydrogen bonded to the anions and/or hydroxylated layers. On gradual heating the loosely bound water is readily eliminated while it will be slightly more difficult to free the second hydrogen bonded ones.

In the event of a grafting process, this second weight loss associated to water would then result from condensation of chromate anions on the brucite-like sheets. Such a step is not visible with [Ni–Al–Cr_2O_7] as the grafting seems to proceed instantaneously at lower temperatures rather than gradually, as shown in Fig. 5, and all the interlamellar water is eliminated in a single step in the temperature range 140–220 °C.

The next major weight loss in the LDHs concerns the dehydroxylation process. When comparing the TGA profiles of the LDHs the striking feature is the gradual evolution of this process with the intercalated anion. The chloride precursor collapses at around 290 °C, while the chromate is completely dehydroxylated above 360 °C and the dichromate at the surprisingly high temperature of 470 °C. The existence of a plateau, a range of temperature during which absolutely no thermogravimetric event is observed, indicates a very stable material. This particular behaviour of the dichromate LDH can prove to be a beneficial feature, mainly in catalytic application: structural modification can sometimes greatly influence the catalytic properties of a given material. This is unequivocal evidence of the enhancing of the thermal properties of takovite-like LDHs by the intercalation of chromium oxo-anion. The occurrence of this last weight loss shows that not all the hydroxyl groups are involved in the grafting process. The delay in the complete dehydroxylation of the LDHs may be related to the fact that the remaining OH are either not close enough to undergo condensation or are mobilised in some kind of interaction with the anionic species. We would be more in favour of the second possibility as no free hydroxyls have been evidenced by FTIR. These observations would rather suggest that only a fraction of the total hydroxyls are eliminated *via* a grafting process while the remaining are most probably involved in a network of hydrogen bonds, possibly with the oxygen atoms of the chromate or dichromate anions. These anionic species would thus be acting like a kind of bridge between the OH groups.

Better to investigate the occurrence of a grafting process within the interlayer, the local surroundings of the anion were analysed using X-ray absorption. EXAFS at the nickel K edge was not very effective in this because of the intense second peak (Fig. 3). Indeed, this peak is located at around the same distance where the contribution of the interlayer species is normally expected to be visible. Instead, it is more convenient to carry out the analyses at the chromium K edge in order to follow the change in its environment, as an anionic entity, with increasing calcination temperatures. The Fourier transform EXAFS spectra of the untreated material and that calcined at 150 °C are shown on Figs. 7 and 8. For both chromate and dichromate, no significant variation from the spectra of the 150 °C sample was observed for materials calcined at higher temperatures. In these spectra, the constancy of the first peak clearly evidences that the immediate neighbourhood of chromium is not affected by calcination at 150 °C implying that the chromate and dichromate anions conserve most of their structural characteristics. However, due to thermal excitation and the absence of long range ordering, only this first peak is well defined and intense. Beyond a (non-corrected) distance of about 2 Å the peaks are broad and of very weak intensity, which renders further refinements of the EXAFS signals practically impossible. On the other hand, this demonstrates the lack of a structural arrangement around both anion entities.

In order to limit the effects of thermal excitation, and, hence, to improve the resolution of the peaks above 2 Å, the EXAFS data were also recorded at very low temperature (8 K). For example, in the case of the untreated [Ni–Al–CrO_4] (Fig. 7a), it becomes possible to distinguish two clearly separated peaks,

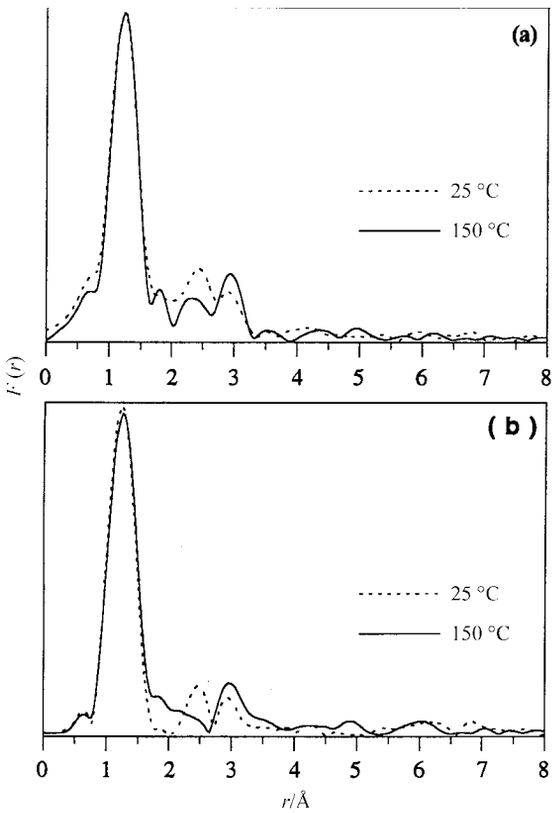

Fig. 7 EXAFS at the chromium K edge of [Ni–Al–CrO_4] for (a) k- and (b) k^3-weighted simulations.

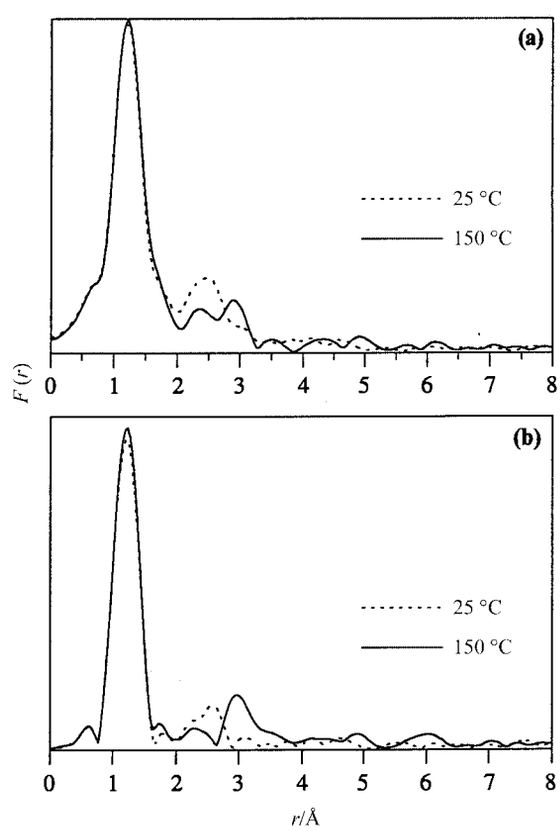

Fig. 8 EXAFS at the chromium K edge of [Ni–Al–Cr_2O_7] for (a) k- and (b) k^3-weighted simulations.

the first one at 2.4 and the other at 2.9 Å. The experimental data were also treated using both k- and k^3-weighted Fourier transform: a treatment using k^3-weighted functions will normally increase any contribution from heavy atoms. With this method, the difference between the atomic numbers of oxygen and other cations (Ni, Al, and Cr) is high enough to distinguish oxygen from the other retrodiffusors' contributions. As the relative intensities of the two maxima do not seem to be affected by the k^3-weighting (Fig. 7b), it suggests that the peaks are most probably due to oxygen atoms. In which case, the one located at 2.4 Å can be assigned to the interlayer water molecules, the first atoms of the brucite-like sheets are well beyond this limit, at around 3.3 Å. This would then suggest the presence of water molecules solvating the anions, as underlined earlier on the basis of thermogravimetric analysis. Regarding the peak at 2.9 Å, it can be attributed either to interlamellar species or to the OH^- from the LDHs framework, knowing that the corrected distance due to phase shift is about 0.4–0.5 Å greater. Given the regular shape and good resolution of the peak, it is more likely to represent the OH^- groups, the positions of which are better defined than those of the surrounding anions or water molecules.

On calcining the material at 150 °C the spectrum is significantly altered in the region between 2 and 3 Å. The difference is further enhanced and becomes more evident when a k^3-weighted Fourier transform is applied. First, there is a considerable weakening of the peak at 2.4 Å following the loss of interlamellar water molecules, which would be in good agreement with the PXRD data and thermogravimetric analyses discussed earlier. Another important feature is observed: the increase of the peak at 2.9 Å. The difference in intensity between the two peaks is now more important. It would be appropriate to assume that this third peak represents the contributions from atoms heavier than oxygen. The grafting of the anions implies a decrease in the distance between chromium and the metallic cations of the LDH sheets, together with the elimination of OH^-. The evolution of this distance, from 4.3 to 3.4 Å for the chromate LDH can be related to the modification of the peak located at 3 Å: the oxygens of the OH groups are then in the first co-ordination shell of chromium and the metallic components of the hydroxylated sheets move closer to chromium.

The same structural modifications are observed with the dichromate containing [Ni–Al], and the evidence for a grafting process is thus reinforced (Fig. 8). The main difference in this sample concerns the peak at 2.4 Å which is more intense than in [Ni–Al–CrO_4]. However, this can be explained by the structural characteristics of the dichromate anion, which consists of two corner-sharing tetrahedra: the proximity of another chromium will affect the atomic distribution around the probe atom.

Analysis of the textural properties of the takovite-like solids has been carried out through the adsorption–desorption isotherms of N_2 at 77 K. The isotherms for the three samples are included in Fig. 9. They all correspond to type IV in the IUPAC classification,[33] a characteristic of mainly mesoporous materials, while the shape of the hysteresis, according to de Boer's classification,[34] is compatible with the structural properties of layered compounds. The measured surface areas and the Brunauer–Emmett–Teller (BET) parameters are summarised in Table 5. It is interesting that pillaring of the parent LDH with chromium oxo-anions results in a decrease of the specific area, while we were expecting a higher surface following the interlayer expansion. However, before being analysed by the adsorption technique the materials had to be cleaned from surface impurities and interlayer water removed to obtain accurate and reproducible results. This step implies a mild calcination in air followed by outgassing of the sample. Given the results observed, it is believed that the measured surface represents mainly the interparticle voids rather than the interlamellar space. Anions adsorbed on the surface of the cystallites will enhance their aggregation, making them more compact and leaving less empty space or limiting the diffusion of the gaseous adsorbate. Although the chloride precursor exhibits the highest crystallinity of the three materials, it also possesses the highest surface area. This can be related to the

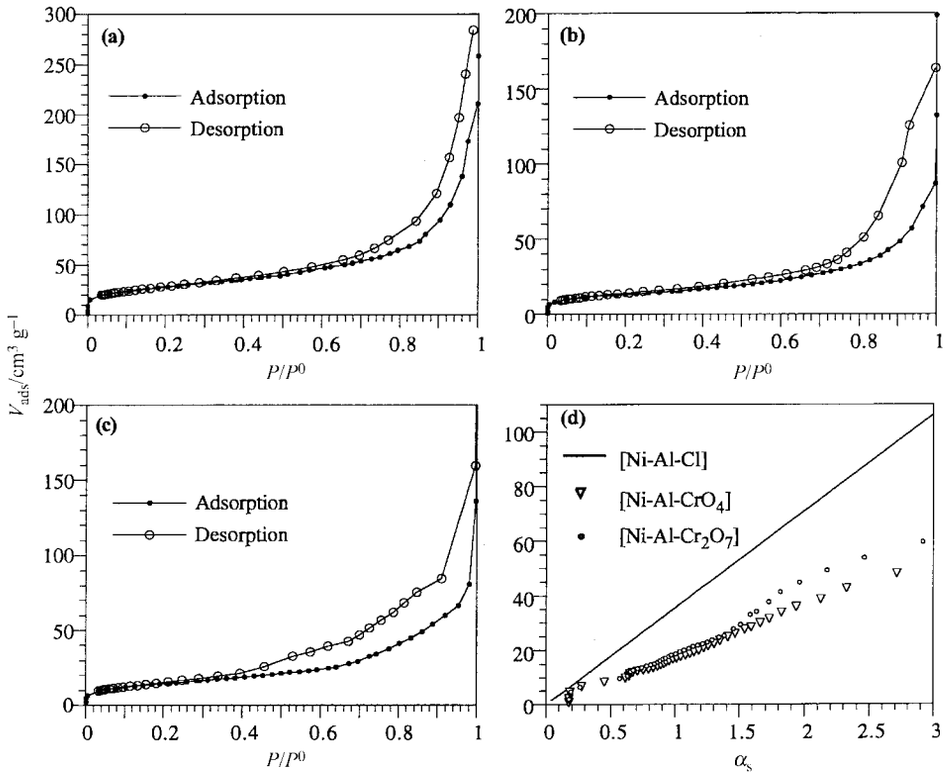

Fig. 9 Nitrogen adsorption–desorption isotherms for (a) [Ni–Al–Cl], (b) [Ni–Al–CrO_4] and (c) [Ni–Al–Cr_2O_7]. The α_s plots of the exchanged materials are compared to that of the parent LDH in (d).

Table 5 BET parameters of [Ni–Al] LDHs

LDH	Monolayer volume, V_m/cm^3	Specific surface area, S_{BET}/m^2 g^{-1}	C_{BET}	Porous volume, V_p/cm^3 g^{-1}
[Ni–Al–Cl]	23.5	98	88	0.399
[Ni–Al–CrO_4]	10.8	47	145	0.205
[Ni–Al–Cr_2O_7]	12.1	53	77	0.210

fact that in this material no grafting process is involved. The α_s plots for the three LDHs are shown in Fig. 9(d), with the chloride precursor being used as reference to study the variation from the parent material. The curves for [Ni–Al–CrO_4] and [Ni–Al–Cr_2O_7] are very similar, hence involving matching microtextural properties, which is not very surprising given their chemical similarity. On the other hand, their common downward deviation from [Ni–Al–Cl] indicates that both anions seem to interact in the same way with the LDH framework to yield close porous structures. However, the difference in the specific surface areas of the pillars is not significant enough to be ascribed to any particular characteristic of the respective anions.

The grafting of oxometalates has previously been reported by several authors dealing with different metal cations in the layer and intercalated anions: [Mg–Al–SO_4],[27] [Zn–Al–CrO_4] and [Zn–Al–Cr_2O_7],[32,35] [Cu–Cr–CrO_4] and [Cu–Cr–Cr_2O_7].[14,36] However, it was mainly on the basis of interlayer contraction (PXRD) and evolution in the symmetry of the anions (FTIR) that these authors suggested the possibility of a grafting process. We have detailed in this work how a wealth of structural information can also be obtained by a combination of thorough thermogravimetric analyses and anion-edge EXAFS spectroscopy, most of which is new. Although the [Cu–Cr] LDHs were also analysed at the chromium K edge by X-ray absorption, the presence of chromium in the layers thwarted the specific study of the chromate and dichromate anions. Whether with [Zn–Al] or [Cu–Cr] LDHs the maximum calcination temperature for which the lamellar structure was reported to be maintained was 200 °C. The takovite-like LDHs are thus proved to be thermally more stable than their homologues. This stability is the result of the conjugate effect of nickel being present in the hydroxylated sheets and the nature of the interlamellar anion.

Conclusion

One of the main objectives of this work was to obtain pillared LDHs by intercalation of inorganic anions in the interlayer domain and through interaction of these entities with the host's framework. The idea was to create three-dimensional structures, with the possibility to modulate the dimensions of these interlayer pores and the chemical properties of the material by a judicious choice of the incoming anion. The physical techniques used to characterise the different properties of anion-exchanged LDHs all show deviations from the typical behaviour of the parent material. In all cases, these deviations can be explained by a grafting process during which the anionic entity, chromate or dichromate, becomes strongly attached to the hydroxylated sheets. Upon mild thermal treatment, a considerable shrinkage of the interlayer is evidenced by PXRD, compatible with the formation of new bonds with the hydroxylated sheets. This phenomenon was further revealed by X-ray absorption (EXAFS), the spectra showing the appearance of new features in the thermally treated samples. Moreover, thermogravimetric analyses have shown that the exchanged LDHs possess a much better thermal stability than that of the chloride precursor; in the best case, the lamellar structure is maintained up to 450 °C.

Generally, the anionic exchange properties of LDHs are maintained after a first exchange, which will limit their application in areas necessitating a liquid, *e.g.* heterogeneous catalysis. The preparation of ready to use materials will thus imply a step which will induce the formation of new bonds between the anions and the LDH framework, strong enough to overcome swelling by hydration or competition from other anions.

We have tried to rehydrate and back exchange (with CO_3^{2-}) calcined [Ni–Al–CrO_4] and [Ni–Al–Cr_2O_7], by re-slurrying the materials in water or an aqueous solution of sodium carbonate, and no interlayer expansion was observed for samples calcined at 150 °C or above. The grafting process is thus permanent.

Acknowledgements

F. M. acknowledges a grant from Université Blaise Pascal, under a BRITE-EURAM project funded by the EC (Contract BREU-CT91-0480). We are grateful to the L.U.R.E. (Laboratoire pour l'Utilisation du Rayonnement Electromagnétique, Orsay, France) for providing access to their EXAFS facilities.

References

1 F. Cavani, F. Trifiro and A. Vaccari, *Catal. Today*, 1991, **11**, 173.
2 R. Allmann, *Acta Crystallogr., Sect. B*, 1968, **24**, 972.
3 S. Bonnet, C. Forano, A. de Roy, P. Maillard, M. Momenteau and J. P. Besse, *Chem. Mater.*, 1996, **8**, 1962.
4 F. Kooli, I. Crespo, C. Barriga, M. A. Ulibarri and V. Rives, *J. Mater. Chem.*, 1996, **6**, 1199.
5 F. Trifiro and A. Vaccari, in *Comprehensive Supramolecular Chemistry*, eds. J. L. Atwood, D. D. MacNicol, J. E. D. Davies and F. Vögtle, Pergamon, Oxford, 1996, vol. 7, ch. 10, pp. 251–291.
6 R. Mokaya and W. Jones, in *Multifunctional Mesoporous Inorganic Solids*, eds. C. A. C. Sequeira and M. J. Hudson, Kluwer, Dordrecht, 1993, p. 425.
7 M. A. Kuehne, H. H. Kung and J. T. Miller, *J. Catal.*, 1997, **171**, 293.
8 F. Malherbe, C. Forano and J. P. Besse, *Microporous Mater.*, 1997, **10**, 67.
9 V. Rives and M. A. Ulibarri, *Coord. Chem. Rev.*, 1999, **181**, 61.
10 M. A. Drezdzon, in *Novel Materials in Heterogeneous Catalysis*, eds. R. Terry, K. Baker and Larry L. Murrel, American Chemical Society, Washington DC, 1990, pp. 141–148.
11 F. Malherbe, C. Forano, M. P. Atkins, B. Sharma and J. P. Besse, *Appl. Clay Sci.*, 1998, **13**, 381.
12 E. C. Kruissink, L. L. van Reijen and J. R. H. Ross, *J. Chem. Soc., Faraday Trans. 1*, 1987, **77**, 649.
13 K. El Malki, A. de Roy and J. P Besse, *Eur. J. Solid State Inorg. Chem.*, 1989, **26**, 339.
14 C. Depège, C. Forano, A. de Roy and J. P. Besse, *Mol. Cryst. Liq. Cryst.*, 1994, **244**, 161.
15 D. E. Sayers, E. A. Stern and F. W. Lyttle, *Phys. Rev. B*, 1971, **27**, 1204.
16 D. E. Sayers, E. A. Stern and F. W. Lyttle, *Phys. Rev. B*, 1975, **11**, 4836.
17 A. Michalowicz, Thèse d'Etat, Université Paris Sud, 1985.
18 L. Châtelet, J. Y. Bottero, J. Yvon and A. Bouchelaghem, *Colloids Surf. A: Physicochem. Eng. Aspects*, 1996, **111**, 167.
19 S. Miyata and A. Okida, *Clay Miner.*, 1977, **25**, 14.
20 M. Bellotto, B. Rebours, O. Clause, J. Lynch, D. Bazin and E Elkaïm, *J. Phys. Chem.*, 1996, **100**, 8527.
21 S. K. Yun and T. J. Pinnavaia, *Chem. Mater.*, 1995, **7**, 348.
22 M. J. Hernandez-Moreno, M. A. Ulibarri, J. L. Rendon and C. J. Serna, *Phys. Chem. Miner.*, 1985, **12**, 34.
23 K. Nakamoto, in *Infrared and Raman Spectra of Inorganic and Coordination Compounds*, Wiley, New York, 1986.
24 R. G. Brown and S. D. Ross, *Spectrochim. Acta*, *Part A*, 1972, **28**, 1263.
25 J. K. Brandon and I. D. Brown, *Can. J. Chem.*, 1968, **46**, 933.
26 O. Clause, B. Rebours, E. Merlen, F. Trifiro and A. Vaccari, *J. Catal.*, 1992, **133**, 231.
27 V. R. L. Constantino and T. J. Pinnavaia, *Inorg. Chem.*, 1995, **34**, 883.
28 T. Hibino, Y. Ymashita, K. Kosuge and A. Tsunashima, *Clays Clay Miner.*, 1989, **43**, 427.
29 M. del Arco, V. Rives and R. Trujillano, *Stud. Surf. Sci. Catal.*, 1994, **87**, 507.
30 M. Bellotto, B. Rebours, O. Caluse, J. Lynch, D. Bazin and E. Elkaim, *J. Phys. Chem.*, 1996, **100**, 8535.
31 F. Kooli, V. Rives and M. A. Ulibarri, *Inorg. Chem.*, 1995, **34**, 5114.
32 M. del Arco, V. Rives, R. Trujillano and P. Malet, *J. Mater. Chem.*, 1996, **6**, 1419.
33 K. W. Sing, D. H. Everett, R. A. W. Haul, L. Moscou, R. Pierotti, J. Rouquerol and T. Sieminiewska, *Pure Appl. Chem.*, 1985, **57**, 603.
34 J. H. de Boer, in *The structure and properties of porous materials*, eds. D. H. Everett and F. S. Stone, Butterworths, London, 1958.
35 C. Forano, A. de Roy, C. Depège, M. Khaldi, F. Z. El Métoui and J. P. Besse, in *Synthesis of porous materials: zeolites*, *clays and nanostructures*, eds. M. L. Occelli and H. Kessler, Marcel Dekker, New York, 1996.
36 L. Bigey, C. Depège, A. de Roy and J. P. Besse, *J. Phys. IV* (*C2*), 1997, 907.

Paper 9/03766G